



# Evaluation of the heat transfer enhancement during pool boiling using low concentrations of Al<sub>2</sub>O<sub>3</sub>-water based nanofluid



Leonardo Lachi Manetti<sup>a</sup>, Mogaji Taye Stephen<sup>a,b</sup>, Paulo Arthur Beck<sup>c</sup>, Elaine Maria Cardoso<sup>a,\*</sup>

<sup>a</sup> UNESP – Univ Estadual Paulista, Department of Mechanical Engineering, Av. Brasil Centro 56, 15385-000 Ilha Solteira, SP, Brazil

<sup>b</sup> FUTA – Federal University of Technology Akure, Department of Mechanical Engineering, School of Engineering and Engineering Technology, PMB 704, Ondo State, Nigeria

<sup>c</sup> TUM – Technical University of Munich, Department of Mechanical Engineering, Chair of Turbomachinery and Flight Propulsion, 85748 Garching, Germany

## ARTICLE INFO

### Article history:

Received 5 December 2016

Received in revised form 16 February 2017

Accepted 13 April 2017

Available online 20 April 2017

### Keywords:

Nanofluids

Nucleate boiling

heat transfer coefficient (HTC)

## ABSTRACT

This study presents experimental results for the heat transfer coefficient during pool boiling of DI water and Al<sub>2</sub>O<sub>3</sub>-water based nanofluid at saturation conditions. Based on these data, an analysis of the heat transfer enhancement due to the nanofluids was performed. The experiments were performed for Al<sub>2</sub>O<sub>3</sub>-water based nanofluid with different volume concentrations (0.0007 vol.% and 0.007 vol.%, corresponding to low and high nanofluid concentration, respectively). A copper surface, with different roughness values ( $R_a = 0.05 \mu\text{m}$ , corresponding to a smooth surface, and  $R_a = 0.23 \mu\text{m}$ , corresponding to a rough surface), was used as test section. The nanoparticle average size was 10 nm and the applied heat flux ranged from 100 to 800 kW/m<sup>2</sup>. For nanofluid pool boiling, it was observed an increase in the heat transfer coefficient up to 75 %, and 15% for the smooth and rough surfaces, respectively, in comparison to that of DI water. According to results, the surface roughness is strongly affected by nanofluid concentration due to the nanoparticle deposition on the heating surface. The results indicate that the use of nanofluids is effective on pool boiling heat transfer, for moderate heat flux and low volumetric concentration.

© 2017 Elsevier Inc. All rights reserved.

## 1. Introduction

The necessity of improving the performance of thermal devices that operate at high heat fluxes, and the growing demand from industries toward producing compact and miniaturized equipment, in particular in the area of microelectronics and microcooling devices, has led to the development of different techniques to improve heat transfer.

Nucleate boiling is the most desirable and efficient regime because high heat flux can be achieved with relatively low wall superheating [1]. Moreover, as compared with the convective heat transfer mechanism, the nucleate boiling presents a higher heat transfer coefficient (HTC) and better performance. Ciloglu and Bolukbasi [2] reported that boiling is one of the most effective heat transfer modes encountered in many industrial applications including power plants, refrigeration systems, heat-exchanger systems, and electronic device cooling systems. This has prompted researchers to try out various methods for enhancing the boiling heat transfer, especially in the nucleate boiling regime.

The boiling heat transfer depends on several factors such as the wall superheating, heating surface materials and morphology,

presence of dissolved gases, thermophysical properties of the working fluid, nucleation sites density, and the frequency of the vapor bubbles. Nayara et al. [3] indicated that a fluid with higher thermal conductivity may improve the heat transfer performance of thermal systems, as conventional fluids used in these systems, including oil, water and ethylene glycol mixture, have low thermal conductivity. Additionally, new technologies are giving rise to higher operating temperatures on even smaller devices, and therefore the necessity of better coolants for extending the service life of electronic and structural components.

One of the alternatives to enhance the thermal conductivity is to adopt nanofluids as the working fluid instead of a conventional fluid. Nanofluids containing homogeneously dispersed solid nanoparticles in a liquid show an enhancement in the thermal conductivity [4–6] and thereby, they have the potential for improving the convective heat transfer [7,8]. According to [9–10], nanofluids are a promising way to enhance the heat transfer due to changes in the base fluid properties such as the thermal conductivity. An international benchmark study [11] revealed that the enhancement in thermal conductivity predicted by the effective medium theory is mainly due to the increase of the heat transfer surface area associated with a large specific surface area of nanoparticles.

The use of nanofluids on nucleate pool boiling has been extensively investigated, as well as the nanoscale structures deposited

\* Corresponding author.

E-mail address: [elainemaria@dem.feis.unesp.br](mailto:elainemaria@dem.feis.unesp.br) (E.M. Cardoso).

## Nomenclature

### Alphabetic

CHF	critical heat flux
EDS	energy dispersive spectroscopy
SEM	scanning electron microscopy
SIP	surface-interaction parameter
HTC	heat transfer coefficient
SS	smooth surface
RS	rough surface
$C_{pl}$	specific heat capacity [kJ/kg K]
$C_{sf}$	Rohsenow's correlation coefficient [-]
$d_p$	particle size [nm]
$g$	acceleration due to gravity [ $m/s^2$ ]
$h$	heat transfer coefficient [ $kW/m^2 K$ ]
$h_{lv}$	latent heat of vaporization [kJ/kg]
$k_c$	copper thermal conductivity [W/m K]
$L$	distance between thermocouples [m]
$N_a$	active nucleation sites density [sites/ $m^2$ ]
$P_{atm}$	atmospheric pressure [kPa]
$Pr$	prandtl number [-]

$q''$	heat flux [ $kW/m^2$ ]
$R_a$	average surface roughness [ $\mu m$ ]
$R_c$	cavity radius [m]
$T_i$	thermocouples temperature [K]
$T_{sat}$	saturation temperature of the fluid [K]
$T_w$	surface temperature [K]

### Greek letters

$\theta$	static contact angle [ $^\circ$ ]
$\rho$	density [ $kg/m^3$ ]
$\sigma$	surface tension [N/m]
$\mu$	viscosity [ $kg/m s$ ]
$\Delta T$	wall superheating [K]

### Subscripts

HTE	heat transfer coefficient enhancement
l	liquid
nf	nanofluid
v	vapor

on the heating surface. However, some conflicting experimental results have been reported on the effect of nanoparticles on the boiling heat transfer with respect to improving the thermal conductivity of the base fluid. For application of nanofluids, especially under pool boiling conditions, most of the studies in the open literature have observed enhancement of the critical heat flux (CHF) [12,13]. Significant boiling heat transfer enhancement has also been reported by [14–17], however contrasting with others that reported large heat transfer deterioration [18–21]. Those results showed inconsistencies even for the same nanoparticles and concentrations under similar experimental conditions. Moreover, a few studies have suggested that differences in the boiling HTC are related to the deposition of nanoparticles on the heating surface [20,22,23].

In Table 1, selected experimental studies from the literature concerning nanofluid pool boiling in the last years are presented. These studies are focused on the evaluation of the HTC and CHF. According to the data in this table, most of studies were performed for  $Al_2O_3$  nanoparticles using copper as heating surface. Experiments were performed for nanoparticles sizing from 15 to 200 nm, and for heating surfaces with different roughness values ranging from 0.005 to 0.42  $\mu m$ .

Ahmed and Hamed [10] showed that the interaction between surface roughness and the nanolayer formed by nanoparticles deposition depends on the nanofluid concentration. Also, deposition of nanoparticles were observed at a slower rate for low nanofluid concentration (0.01 vol.%), resulting in enhancement of the boiling HTC. Based on their experiments performed for the conditions described in Table 1, 35% enhancement of HTC for  $Al_2O_3$ -water based nanofluid on a heated copper block was reported.

Kwark et al. [24] observed a deterioration of about 22% in the HTC. Those authors indicated the Alumina-water nanofluid caused a critical layer condition, corresponding to the maximum limit of the surface wettability reflected by a constant CHF. According to them, additional nanoparticle layers could increase the coating thickness, thus providing a barrier to heat transfer which may cause a reduction in the number of microcavities and an increase in the thermal resistance of the heating surface. Shahmoradi et al. [25] also reported a decrease in the HTC by adding alumina nanoparticles to pure water (for concentrations values 0.001, 0.002, 0.02, 0.05 and 0.1 vol.%), in order to analyze the nanofluid pool boiling behavior and the effect of surface characteristics on

the HTC and the CHF. According to them, for very low nanofluid concentration, such as 0.001 vol.%, the changes in the HTC were not significant.

In order to avoid the nanoparticle deposition and to improve the stability of the liquid solution, Tang et al. [26] performed boiling experiments with  $Al_2O_3$  - R141b, at concentrations of 0.001 vol.%, 0.01 vol.% and 0.1 vol.% with and without surfactant SDBS. According to them, the presence of the surfactant increased the HTC for higher particle concentrations (0.01 vol.% and 0.1 vol.%) because the surfactant strongly reduces the deposition of nanoparticles. An enhancement of the HTC in 22% was also reported by Kole and Dey [6] at low ZnO-ethylene glycol concentration as compared to pure ethylene glycol. However, a degradation of the HTC was observed at higher ZnO-ethylene glycol concentration. According to those authors, the degradation of the HTC at higher nanofluid concentration occurred due to the active nucleation sites blockage by sedimentation of nanoparticle.

The HTC enhancement/deterioration conflicting behavior was also reported by [6,10,27–29]. In general, the authors observed that the nanoparticles deposition onto the heating surface during nanofluid pool boiling was the main cause of changes in the HTC and CHF. Lee et al. [30] studied the effect of magnetite-water based nanofluid on the CHF, for three different low nanofluid concentrations. Another two types of nanoparticles (alumina and titanium) were prepared for the pool boiling CHF experiments using the same concentrations of magnetite. According to Lee et al. [30], the CHF increased for all cases, and the CHF for magnetite-water based nanofluid showed the highest value among the evaluated nanofluids. The authors emphasized the importance of the surface wettability and the surface tension as the parameters responsible for the enhancement of the CHF.

Vafaei [31], based on the experimental conditions described in Table 1, observed a decrease in the HTC with increasing nanofluid concentration for smooth heating surface as compared to pure water, whereas for rough heating surface 140% enhancement in the HTC was observed for similar nanofluid concentration at both low and high heat flux conditions. That author inferred that the highest HTC found for low heat flux values may be due to the nanoparticles deposition on the heating surface which can lead to an increase of the surface roughness. As the heat flux increases, the nanolayer thickness on the heating surface also increases, leading to degradation of the HTC because of the surface roughness

**Table 1**  
Literature review of some nanofluid heat transfer experimental studies performed in the last years.

Authors	Nanofluid characteristic	Surface material and roughness	CHF effect	HTC effect	Surface roughness after boiling
Ahmed and Hamed [10]	Alumina (40 nm) in water	Copper plate, $R_a = 50$ nm	Not reported	Enhancement/deterioration <sup>a</sup>	Increased
Kwark et al. [24]	Alumina (139 nm) in water	Copper plate	Enhancement	Unchanged/deterioration <sup>a</sup>	Not reported
Shahmoradi et al. [25]	Alumina (40 nm) in water	Copper plate, $R_a = 5.1$ nm	Enhancement	Deterioration	Increased
Vafaei [31]	Alumina (20–150 nm) in water	Copper plate, $R_a = 25$ nm and $R_a = 420$ nm	Not reported	Enhancement/deterioration/unchanged <sup>a</sup>	Increased for $R_a = 25$ nm, decreased for $R_a = 420$ nm
Sarafraz et al. [32]	Alumina (20 nm and 50 nm) in water	Copper plate	Enhancement	Enhancement	Not reported
Tang et al. [26]	Alumina (20–200 nm) in R141b with and without surfactant (SDBS)	Copper plate	Not reported	Enhancement (with SDBS), deterioration (without SDBS)	Not reported
Sarafraz and Hormozi [27]	Alumina (45–50 nm) in ethylene glycol	Stainless steel cylinder, $R_a = 54$ nm	Not reported	Deterioration	Decreased
Sarafraz and Hormozi [28]	Copper oxide (50 nm) in water with and without surfactant (SDS)	Stainless steel cylinder, $R_a = 340$ nm	Not reported	Enhancement (with SDS), deterioration (without SDS)	Decreased
Kathiravan et al. [29]	Copper (20 nm) in water with and without surfactant (SDS)	Stainless steel plate, $R_a = 167$ nm	Enhancement (without SDS), deterioration (with SDS)	Deterioration	Decreased
Lee et al. [30]	Magnetite (25 nm) in water	Ni-Cr wire	Enhancement	Not reported	Not reported
Kole and Dey [6]	Zinc oxide (30–40 nm) in ethylene glycol	Copper plate, $R_a = 90$ nm	Enhancement	Enhancement	Increased

<sup>a</sup> Depending on nanofluid concentration.

enhancement due to the nanoparticle deposition counterbalancing the thermal resistance of the nanoparticle deposited layer.

According to Sarafraz et al. [32] the nanoparticle deposition on the heating surface can increase the surface wettability which reduces the nucleation sites density and, consequently, degrading the HTC. Besides, Ciloglu and Bolukbasi [2] pointed out that the main reason for the enhancement of the CHF and for the degradation of HTC by using nanofluids during pool boiling is due to the changes in the heating surface morphology, i.e., a decrease of active nucleation sites and also, of the contact angle. However, for low nanofluid concentrations, the nanoparticle deposition can also contribute to creating new nucleation sites, leading to the HTC improvement. Consequently, more systematic researches are needed to fully understand the mechanisms associated with the HTC enhancement (or degradation) in the pool boiling of nanofluids.

In this study, an experimental investigation was performed for pool boiling of deionized (DI) water and  $Al_2O_3$ -water based nanofluid at saturated conditions, in order to analyze the influence of low nanofluid concentrations on the HTC behavior. Based on the contradictory results provided by the literature for the HTC, this paper aims to clarify the influence of nanoparticle deposition and nanofluid concentration on the pool boiling heat transfer, and also, to point out the mechanisms responsible for the heat transfer enhancement.

## 2. Experimental apparatus and procedure

### 2.1. Heating surface and nanofluid preparation

The boiling tests were performed on copper heating surfaces of 20 mm diameter. Initially, the surfaces were polished in order to obtain different surface roughnesses, one corresponding to a smooth surface ( $R_a = 0.05$   $\mu$ m, namely SS), and another one to a rough surface ( $R_a = 0.23$   $\mu$ m, namely RS). The smooth surface was manufactured mechanically by polishing the copper surface using an aluminum-oxide abrasive compound, while the rough surface

was manually polished using a #600 emery paper. Prior to the pool boiling testing, all heating surfaces were cleaned with acetone and dried using an air jet.

This study has been carried out with  $Al_2O_3$ -water based nanofluid prepared by the two-step method that involves weighting the dry nanoparticles and subsequently dispersing them into DI water. Aluminium oxide nanoparticles, with an average particle size of 10 nm were used in this experiment. Two nanofluid concentrations of 0.0007 vol.% and 0.007 vol.% (corresponding to low and high nanofluid concentration, respectively) were tested. Ultrasonication was performed for 3 h (25 kHz) to obtaining a uniformly dispersed solution. No surfactant was used in this experiment, and no sedimentation was observed for 48 h after preparing the nanofluids.

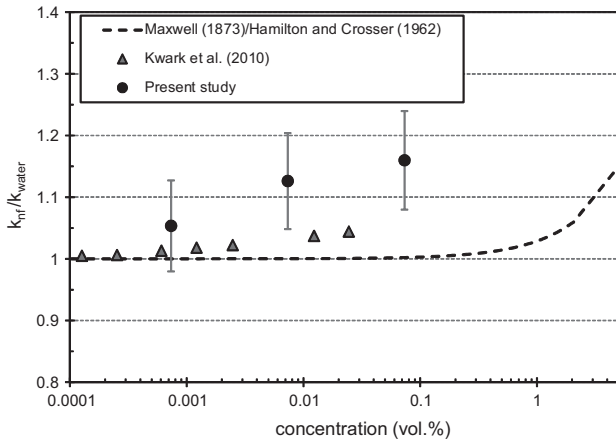
The thermal conductivity of the nanofluids was evaluated using the transient hot wire method (Hukseflux TP-08 probe) at 300 K. The transient hot wire method measures the temperature response of the wire with time for an electrical power. From these measurements, it was concluded that the variation of the thermal conductivity was only marginal (values found close to the thermal conductivity of water, as shown in Fig. 1) and within the error band of the equipment,  $\pm 3\%$ .

Due to the low volumetric concentrations of the nanofluid used in the present study, this behavior was already expected and it is in agreement with the measurements of Kwark et al. [24], and the predictive methods of Maxwell [33] and Hamilton and Crosser [34] with a maximum error of 12%.

### 2.2. Pool boiling experimental setup

Fig. 2 pictures the pool boiling apparatus, where a glass cube (boiling chamber) with a thickness of 5 mm and dimensions  $170 \times 170 \times 180$  mm involves a borosilicate glass tube of internal diameter 90 mm, height of 180 mm and wall thickness of 10 mm.

The external chamber and the boiling chamber was fixed between two plates of stainless steel AISI 316 with dimensions of



**Fig. 1.** Effect of the volume nanofluid concentration on the effective thermal conductivity ratio of  $\text{Al}_2\text{O}_3$ -water based nanofluid ( $T = 300 \text{ K}$ ).

$200 \times 200 \times 10 \text{ mm}$ . Nitrile rubber and silicone was used for sealing the boiling chamber. In the gap between the boiling chamber and the external wall, there was a forced flow of water that kept the working fluid inside the boiling chamber near the saturation point ( $T_{\text{sat}} = 99 \text{ }^\circ\text{C}$ ). A second thermostatic bath was used to control the temperature of the condenser located at the top of the boiling chamber (Fig. 3).

Two K-type thermocouples located in the boiling chamber allowed monitoring the temperature of both the working fluid and vapor. The pressure inside the boiling chamber was measured by a pressure transducer, and maintained at 98 kPa (local atmospheric pressure,  $p_{\text{atm}}$ ) during the boiling tests.

The test section consisted of a copper block (20 mm diameter and 60 mm height) containing three K-type thermocouples to estimating the wall temperature and the heat flux. The thermocouples plugged into 1 mm diameter holes (filled with copper powder to avoid air gaps) at the radial center of the copper cylinder. The copper block was heated by a cartridge resistance capable of providing a maximum heat flux of  $1100 \text{ kW/m}^2$ . The thermal insulation of the test section consisted of 40 mm thick layers of polytetrafluoroethylene and vermiculite.

### 2.3. Experimental procedures

The experiments were performed using DI water or  $\text{Al}_2\text{O}_3$ -water based nanofluid under saturated conditions at 98 kPa. The same

procedure was adopted during all trials in order to ensure repeatability.

Before each run, the working fluid was heated very close to the saturation temperature in order to degas it. Vacuum was created in the boiling chamber prior to feeding the chamber with the working fluid. The test conditions were regulated by monitoring the pressure and the temperature inside the boiling chamber.

Saturated conditions were assured by keeping the difference between the fluid temperature inside the boiling chamber, and the saturation temperature (estimated from the measured pressure) within a range of  $\pm 0.4 \text{ }^\circ\text{C}$ . Furthermore, all tests were conducted with the same volume of the working fluid (200 ml) and, consequently, the same height of fluid column ( $\approx 30 \text{ mm}$ ).

Once the test conditions stabilized, the heat flux was imposed in the range from 100 to  $800 \text{ kW/m}^2$  by increasing the electrical power. The stable condition was characterized by variations on the temperature within the uncertainty of their measurements ( $\pm 0.4 \text{ }^\circ\text{C}$ ). The heat flux and the surface temperature were calculated using the 1-D conduction law of Fourier with the readings from the thermocouples embedded in the copper block. The temperature of the surface in contact with the working fluid was then determined by extrapolating the linear temperature profile to the upper surface,  $T_w$ . The copper block and the location of the thermocouples are shown in Fig. 4.

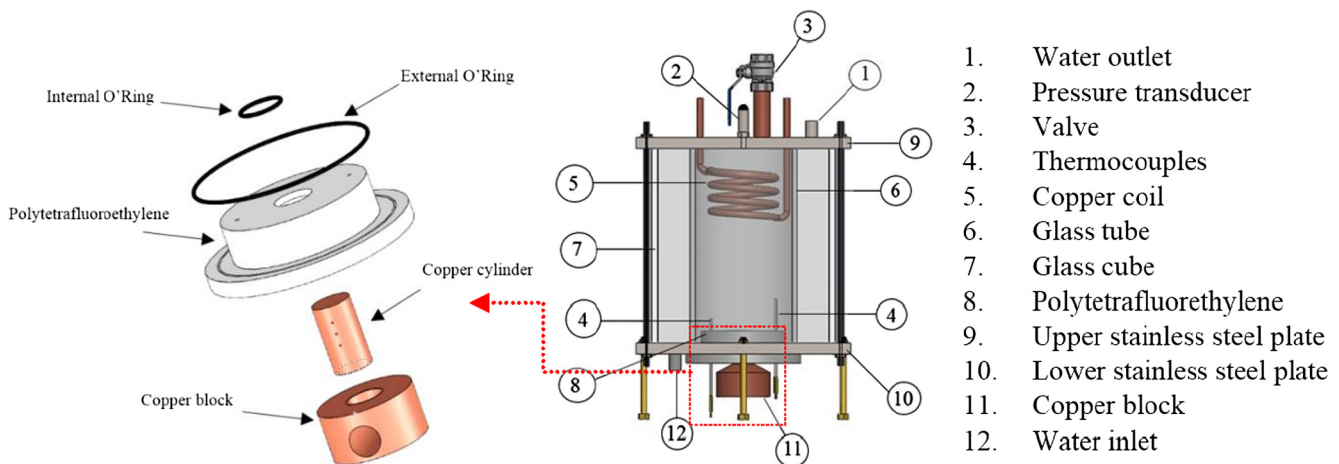
The temperature readings were acquired from the thermocouples by a data acquisition system (Agilent 34970A). Based on the temperature measurements, provided by the thermocouples embedded in the copper block, different curve fittings were obtained for each heat flux (Fig. 5).

The curve fittings were obtained with R-square higher than 0.99. The assumption of negligible heat losses in the radial direction done by Kiyomura et al. [35] seemed suitable for this work, otherwise a linear profile would not fit the experimental data. Besides, the comparison between the imposed heat flux based on the electrical current and voltage measurements, and the heat flux estimated from the linear profile indicated heat losses always lower than 12%, as shown in Fig. 5b.

### 2.4. Data reduction

In this study, the HTC was calculated using the Newton's law of cooling given by

$$h = \frac{q''}{\Delta T} = \frac{q''}{T_w - T_{\text{sat}}(p_{\text{atm}})} \quad (1)$$



**Fig. 2.** Pool boiling apparatus and test section assembly.

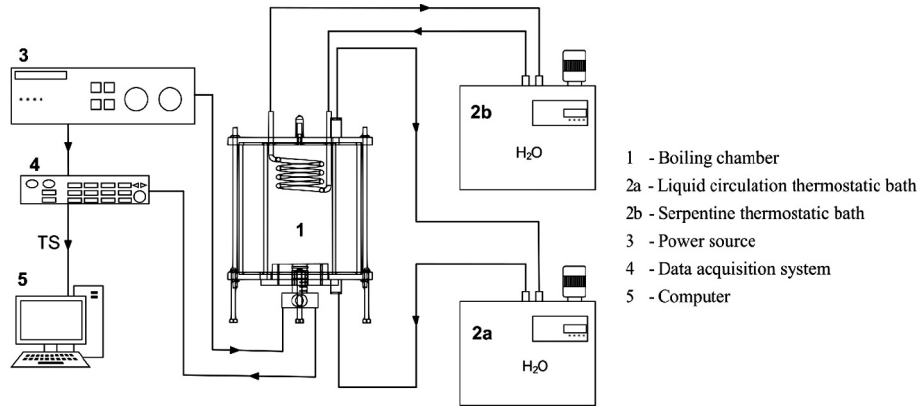


Fig. 3. Schematic diagram of the pool boiling apparatus.

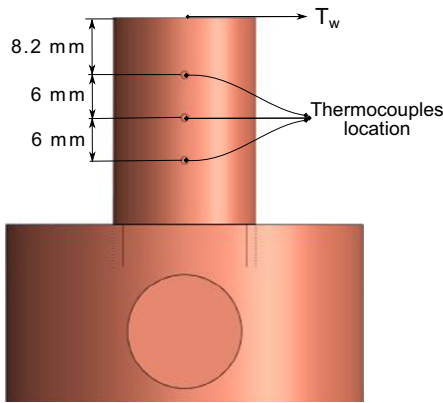


Fig. 4. Copper heater block and thermocouples location.

where  $T_w$  is the wall temperature and  $T_{sat}(p_{atm})$  corresponds to the saturation temperature of the water at atmospheric pressure (98 kPa).

In order to ensure the steady state regime was achieved, each test had a duration of 1500 s for each applied heat flux, but only the temperature data for the last 500 s (corresponding to 100 experimental data points) of the test interval were considered. Applying the same method used by Taylor and Kuyatt [36], the uncertainty of the temperature measurement was  $\pm 0.4^\circ\text{C}$  and, based on the linear curve fitting and the uncertainties of tempera-

ture measurements and the distances among thermocouples and upper surface, the uncertainty of wall temperature was found lower than  $\pm 0.5^\circ\text{C}$ . For all surfaces tested, the experimental uncertainty for the heat flux and for the HTC varied from 1.7% to 15.0%, and from 3.1% to 17.5%, respectively.

2.5. Surface characterization

The heating surface was analyzed using the different techniques, prior and after each boiling test:

- Structural and chemical information by scanning electron microscopy (SEM) and energy dispersive spectroscopy (EDS), performed by the EVO LS15 Zeiss® with a magnification of 1000×;
- Average surface roughness ( $R_a$ ), with the same scanning area for all surfaces, by a Mitutoyo Surftest SJ 301 model with measuring range of  $-200\ \mu\text{m}$  to  $+150\ \mu\text{m}$  (uncertainty of  $\pm 0.005\ \mu\text{m}$ );
- Static contact angles measure by analysis of pictures of a sessile droplet (at  $25^\circ\text{C}$ ) with a mean absolute error (MAE) lower than  $1^\circ$ .

The apparatus used to measure the static contact angle consists of an aluminum plate where the test surface is fixed, a camera, a green LED light source and a light diffuser. The pictures were analyzed using image post processing software to shape the deionized water droplet, as detailed in Kiyomura et al. [35] and Netto et al. [37].

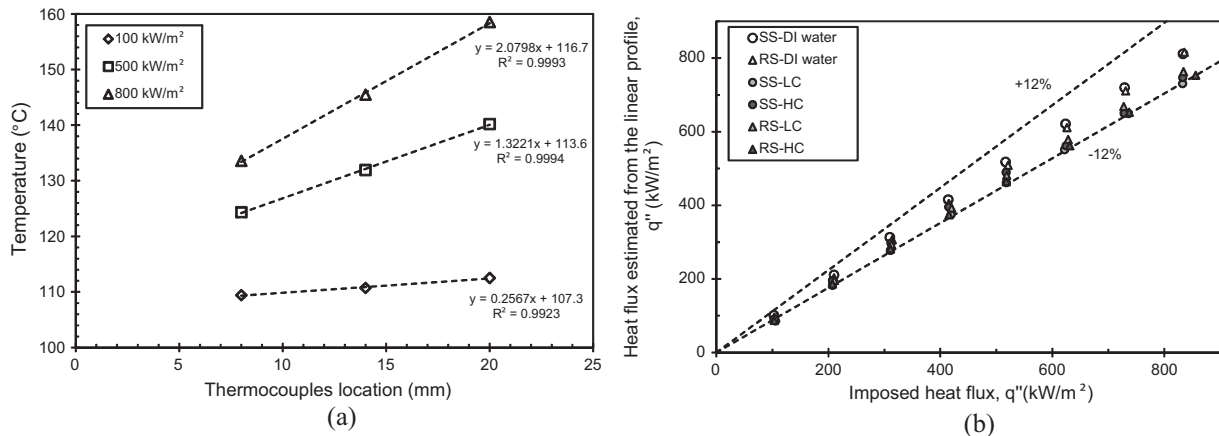


Fig. 5. (a) Linear temperature profiles used to estimate the heat flux and wall temperatures for heat flux of 100, 500 and 800 kW/m<sup>2</sup>, for smooth surface (SS) and DI water as working fluid. (b) Imposed heat flux versus the heat flux estimated from the linear profile.



### 3. Results and discussions

#### 3.1. Validation of the experimental apparatus

In order to validate the pool boiling apparatus, tests were carried out for DI water on the smooth (SS) and rough (RS) heating surfaces. The experimental values, the curve fitting, and the predicted values are plotted in Fig. 6. The curve fitting was based on the relation between the heat transfer coefficient and the heat flux, expressed as

$$h = Cq^n \quad (2)$$

where  $C$  is a coefficient dependent on the surface-fluid interaction, and  $n$  is an exponent of the heat flux. The predicted values of the heat transfer coefficient are given by the Rohsenow's correlation [38],

$$h = \frac{1}{C_{sf}} Pr_l^{-s} \frac{q'' c_{pl}}{q''} \left( \frac{\mu_l h_{lv}}{q''} \right)^r \left[ \frac{\sigma}{g(\rho_l - \rho_v)} \right]^{-r/2} \quad (3)$$

where  $s = 1$  and  $r = 1/3$  for water and,  $\mu_l$ ,  $h_{lv}$ ,  $c_{pl}$ , and  $Pr_l$  represent the viscosity of the liquid (kg/m s), the latent heat of vaporization (J/kg), the specific heat of the liquid (J/kg K), and the Prandtl number of the liquid, respectively.  $C_{sf}$  is a coefficient that depends on the material of the heating surface, and on the surface roughness. The thermo-physical properties of the working fluid were obtained at  $p_{sat} = 98$  kPa.

Following Vachon et al. [39] suggestion,  $C_{sf}$  values of 0.0128 and 0.0092 were adopted for the SS and RS settings, respectively. As shown in Fig. 6, the predicted values agree well with the experimental data with a mean absolute error (MAE) of about 8% for smooth surface, and 11% for rough surface. It can be noticed that the value of  $n$  obtained with Eq. (2) is about 0.6, agreeing with Stephan [40] who reported that, in the nucleate boiling regime, the value of  $n$  generally lies between 0.6 and 0.8.

#### 3.2. Results for the pool boiling of nanofluids

Fig. 7 presents the experimental data for the HTC as function of heat flux in the nucleate boiling regime [41]. The tests were performed for DI water, and for  $Al_2O_3$ -water based nanofluids (at low and high concentration, LC and HC, respectively). Copper surfaces with different roughness values (SS and RS, corresponding to smooth and rough surfaces, respectively) were used as heating surfaces. Due to the fact that the tests were performed for the fully developed boiling regime, it was not possible to visualize the bubble frequency and the departure diameter of the vapor bubbles.

Thus, the authors based their analysis on the heat fluxes and the wall temperature behaviors.

According to Fig. 7, the highest increase in the HTC (up to 75%) as compared to the HTC of DI water on smooth surface is obtained with the smooth surface with low nanofluid concentration (SS-LC) for heat fluxes under  $400 \text{ kW/m}^2$ .

This behavior is caused by the deposition of nanoparticles on the heating surface which in turn leads to an increased surface roughness (Fig. 8a). Moreover, from a certain heat flux threshold, the HTC degrades as the thermal resistance of the nanolayer increases (Fig. 8b), being these observations consistent with those reported by Vafaei [31].

For the rough surface, a slight enhancement (of about 15%) in HTC was observed for the low nanofluid concentration as com-

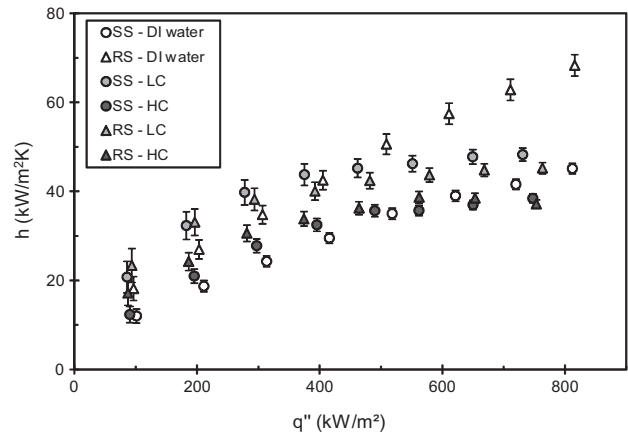


Fig. 7. Comparative analysis between the HTC for DI water and  $Al_2O_3$ -water based nanofluids, for different volumetric concentrations and surface roughnesses.

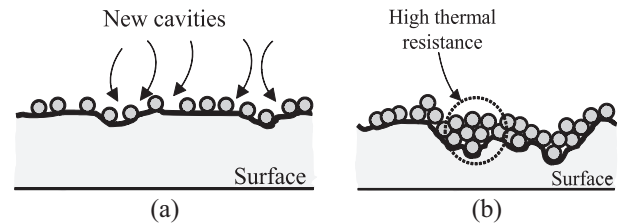


Fig. 8. Schematic drawing of nanoparticles deposition onto the heating surface. (a) smooth surface and (b) rough surface.

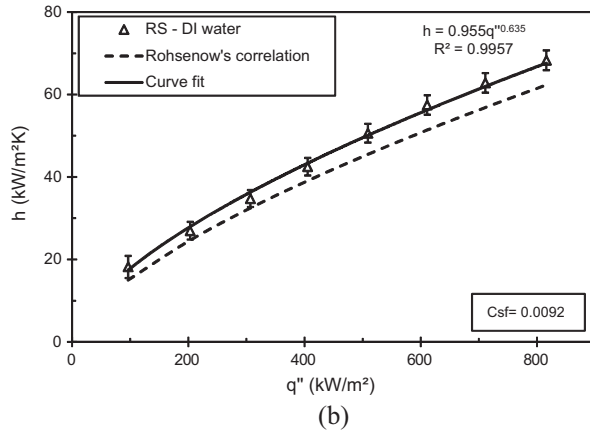
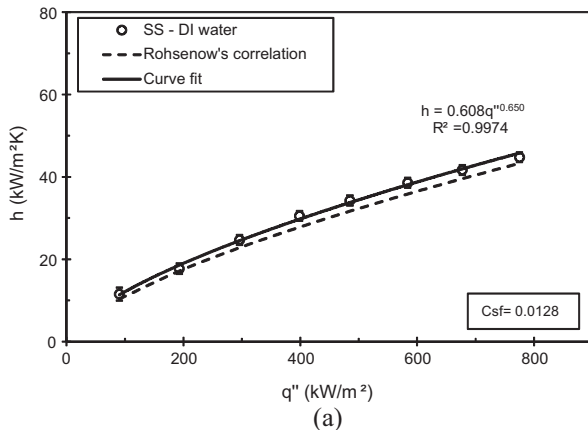


Fig. 6. Pool boiling apparatus validation. (a) smooth surface, SS and (b) rough surface, RS.

pared to the rough surface boiled with DI water. This enhancement occurred for heat fluxes up to 400 kW/m<sup>2</sup>, the threshold from where the HTC sharply drops as a consequence of the increased nanoparticle deposition rate, which reduces the cavity radius and increases the thermal resistance of the heating surface, as schematically shown in Fig. 8b.

Fig. 9 shows the pool boiling curves for DI water and Al<sub>2</sub>O<sub>3</sub>-water based nanofluid with different concentrations (0.0007 vol.% and 0.007 vol.%) on smooth and rough surfaces. As the nanofluid

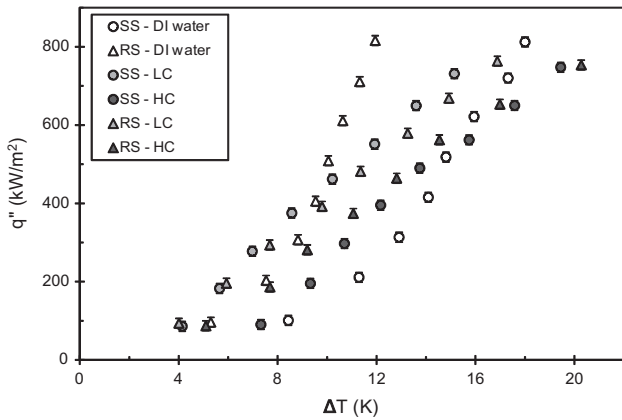


Fig. 9. Pool boiling curves for DI water and Al<sub>2</sub>O<sub>3</sub>-water based nanofluid (at 0.0007 vol.% and 0.007 vol.%) on the smooth and rough surfaces.

concentration increased, the deterioration in the HTC became evident by an increase in the wall superheating, ΔT, regardless of the original surface roughness. The same behavior can be observed in Fig. 7, where the HTC decreased as the concentration of the nanofluids increased.

According to Park et al. [23], most of the heat exchangers operate under heat flux values lower than 200 kW/m<sup>2</sup>. It is worth mentioning that, for both smooth and rough surfaces and for heat fluxes lower than 400 kW/m<sup>2</sup>, enhancements in the HTC due to the addition of Al<sub>2</sub>O<sub>3</sub>-water based nanofluid at low concentrations were achieved in this study.

### 3.3. Effects of the nanoparticle deposition

The nanofluid boiling mechanism proposed by Kim et al. [42] considers that a nanocoating forms during the boiling of the nanofluid as the microlayer underneath the growing vapor bubble evaporates, leaving behind nanoparticles adhered to the heating surface as it is shown in Fig. 10. This nanolayer changes the morphology of the heating surface, and its thickness varies with the nanofluid concentration. Also in Fig. 10, the surface condition is shown for smooth and rough copper surfaces, before and after the pool boiling experiments with different volumetric concentrations of a Al<sub>2</sub>O<sub>3</sub>-water based nanofluid. One may observe that, as the nanofluid concentration increases, the thickness of the nanolayer on the heating surface also increases alongside with the surface roughness, being this effect more pronounced for the smooth surface (SS).



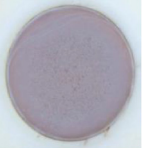
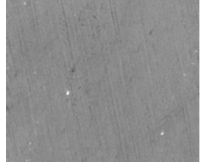
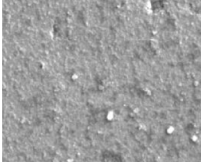
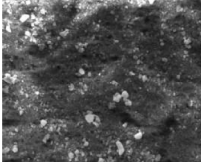
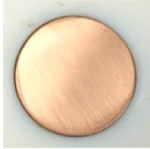

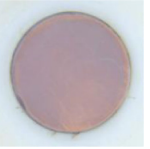
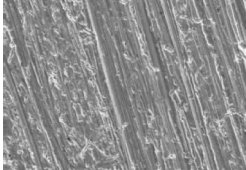
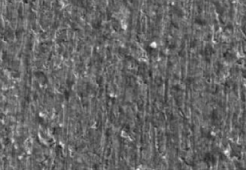
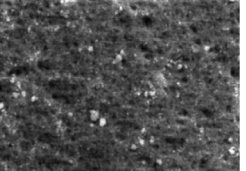
Surfaces	Before nanofluid boiling	After nanofluid boiling (low concentration)	After nanofluid boiling (high concentration)
Smooth surface (SS)	 $R_a = 0.05 \mu\text{m}$ $\theta = 95^\circ$	 $R_a = 0.24 \mu\text{m}$ $\theta = 38^\circ$	 $R_a = 0.61 \mu\text{m}$ $\theta < 10^\circ$
			
Rough Surface (RS)	 $R_a = 0.23 \mu\text{m}$ $\theta = 75^\circ$	 $R_a = 0.28 \mu\text{m}$ $\theta = 35^\circ$	 $R_a = 0.69 \mu\text{m}$ $\theta < 10^\circ$
			

Fig. 10. Surface characteristics and SEM images of smooth and rough surfaces before and after nanofluid pool boiling with different volumetric concentrations.

In order to predict the active nucleation sites density,  $Na$ , and to evaluate the morphology changes due to the nanoparticles deposition observed in this work, an analysis was carried out using the Wang and Dhir's model [43]. In this model, the density (in sites/ $m^2$ ) is given by

$$Na = 7.81 \times 10^{-29} (1 - \cos \theta) R_c^{-6} \quad (4)$$

where  $R_c$  is the cavity radius, i.e., the minimum radius for a cavity to become active, and  $\theta$  is the experimental static contact angle as detailed in Kiyomura et al. [38]. For the smooth and rough surfaces after nanofluid boiling at high concentration, SS-HC and RS-HC, respectively,  $\theta = 10^\circ$  was adopted. The  $R_c$  was estimated using the Griffith and Wallis [44] model,

$$R_c = \frac{2\sigma T_{sat}}{(T_w - T_{sat})\rho_v h_{lv}} \quad (5)$$

where  $T_w$  corresponds to the wall temperature, and  $T_{sat}$  corresponds to the saturation temperature of the water at 98 kPa.

Fig. 11 plots the cavity radii versus heat flux range for surface roughness/working fluid (either DI water or  $Al_2O_3$ -water based nanofluid) settings. One may observe in Fig. 11a that the cavity radius for the SS-LC setting was greater than those of the other settings, this observation indicating that less energy (wall superheating) was required to activate cavities. Therefore, for the same heat flux, a lower wall superheating was achieved with lower concentration nanofluids.

The analysis of the cavity radii for the rough surfaces is pictured in Fig. 11b. The results for the RS-HC settings showed the same trend of the smooth surface settings up to 400  $kW/m^2$ . However, for heat fluxes higher than this value, the cavities got filled with nanoparticles more quickly because of the increased deposition rate, causing a higher wall superheating to maintaining cavities with smaller mouth diameter active. This implies a lower HTC as compared to the RS-DI water setting.

Fig. 12 shows the active nucleation sites density as a function of the heat flux for the surface/working fluid settings used in this work. It can be noticed that both SS-DI water and RS-DI water settings had more nucleation sites than the respective settings for surfaces boiled with nanofluids, and the SS-DI water setting had the highest number of active nucleation sites. This trend is different from that observed in Fig. 7, where the SS-DI water setting had the lowest HTC, i.e., the highest wall superheating. Such behavior can be explained by the fact that the number of active nucleation sites, estimated with Eq. (4), is more strongly influenced by the cavity radius than by the wettability, represented by the contact angle  $\theta$  in that equation.

By comparing the HTC curves in Fig. 7, the cavity radius predicted by Eq. (5) (Fig. 11), and the number of active nucleation sites predicted by Eq. (4) (Fig. 12), one may draw conclusions about the predominant effects on the HTC. The cavity radius seems to play a more important role on the heat transfer behavior, as for the same heat flux, larger cavity radii require less energy (i.e., wall superheating) to be activated, this conclusion upholding the higher HTC values reported in this study. Therefore, contrasting with the

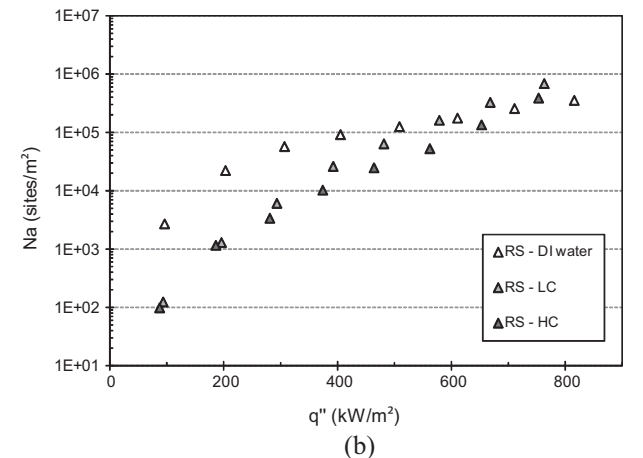
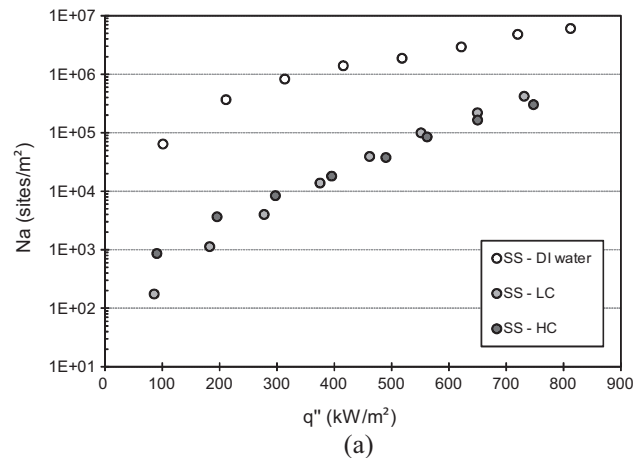
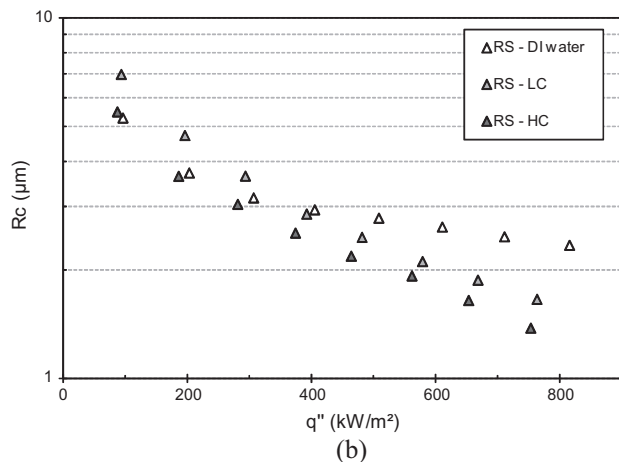
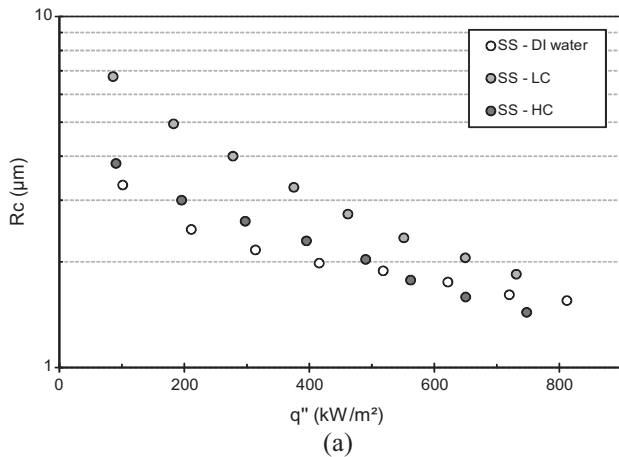


Fig. 11. Effect of heat flux and surface/working fluid on the cavity radius. (a) smooth surface and (b) rough surface.

Fig. 12. Effect of heat flux and surface/working fluid on the active nucleation site density predicted by Eq. (4). (a) Smooth surface and (b) rough surface.



findings of Ciloglu and Bolukbasi [2], the number of active nucleation sites is not the predominant effect on the HTC curves for nanofluids.

In order to show more clearly the effect of the nanofluid concentration on the enhancement/deterioration of the HTC, the experimental results were evaluated using the heat transfer enhancement ratio ( $h_{HTE}$ ), given by

$$h_{HTE} = \frac{h_{nf}}{h_{water}} \quad (6)$$

where  $h_{nf}$  is the heat transfer coefficient of the  $Al_2O_3$ -water based nanofluid, and  $h_{water}$  is the HTC of the DI water. With this purpose, the results of Ahmed and Hamed [10] were compared with the ones in this study for the same surface roughness  $R_a = 0.05 \mu m$ , as shown in Fig. 13. In Fig. 13, the  $h_{HTE}$  decreases with increasing heat flux and nanofluid concentration. It should be noted that the nanofluid with the highest concentration (0.007 vol.%) in this study presents the same behavior of lowest nanofluid concentration (0.01 vol.%) reported by Ahmed and Hamed [10]. This trend indicates a mild effect of the nanoparticle size on the heating surface for low nanofluid concentration, as the nanoparticle size tested by the latter authors was four times larger than the one in this study. It should be noticed that for a moderate heat flux, the  $h_{HTE}$  increases with the heat flux until a threshold value, and from there sharply decreases with increasing heat flux. As pointed out in Section 3.2, for high heat flux the nanoparticles deposition rate may increase, affecting the HTC. However, for the  $Al_2O_3$ -water based nanofluid with 0.5 vol.% used by Ahmed and Hamed [10], it was found that  $h_{HTE} < 1$ , which means a decrease of the boiling performance. This may be related to differences in the surface characteristics and nanofluid concentration considered in their study.

According to Narayan et al. [22], when the surface interaction parameter ( $SIP$ ), which is defined as the ratio between the surface roughness  $R_a$  and the particle size  $d_p$ , was greater than 1, an enhancement of the HTC was observed, and this enhancement occurred due to the deposition of nanoparticles in the cavities, causing a single active cavity to split into multiple ones. For the smooth and rough surfaces considered in the present study, the  $SIP$  values are 5 and 23 respectively. Therefore, in this study  $SIP > 1$  for the smooth surface, and  $SIP \gg 1$  for the rough one. In the study of Ahmed and Hamed [10],  $SIP = 1.25$ , and it becomes evident that the concentration of the nanofluid plays a key role in the boiling effectiveness. The deposition of nanoparticles at a slower rate (i.e., for a heat flux lower than  $400 \text{ kW/m}^2$ ) for the low nanofluid concentration (0.0007 and 0.007 vol.%) settings of this study is the main reason for the higher HTC as compared to the low nanofluid concentration (0.01 vol.%) used by Ahmed and Hamed

[10]. The HTC degradation for 0.5 vol.% nanofluid concentration reported by the latter authors is due to the reduction in the cavities radii caused by the deposition of nanoparticles on the heating surface. For high nanofluid concentration, the nanoparticles fill the cavities at a higher rate and, consequently, a higher wall superheating is necessary to maintaining active cavities with smaller mouth diameter. Besides that, the thickness of the nanolayer on the heating surface provides a barrier to heat transfer which causes an increased thermal resistance.

It is worth mentioning that the literature is still in conflict whether nanoparticles can enhance or degrade the boiling heat transfer, as presented by the authors in Table 1. The main cause of modification in the HTC for nanofluid pool boiling is the deposition of nanoparticles on the heating surface. Therefore, the nanofluid pool boiling heat transfer is strongly affected by the relative size between the nanoparticles suspended in the base fluid, and the heating surface geometry and their interactions. It is clear that in depth research focusing on these interactions, and the bubble growth dynamic in nanofluids is required to fully understand the nanofluid boiling phenomena.

Consequently, we recommend that further studies should take into account the experimental evidences from this work. Firstly, it is advisable to use nanofluids at concentrations lower than 0.001 vol.% to avoid nanoparticle deposition that would lead to increased thermal resistance, and deterioration of the HTC due to the formation of a nanolayer. In addition, smooth heating surfaces coupled with low nanofluid concentration seems to be the best combination to increase the HTC in comparison to that of DI water, this phenomenon being explained by the increase of the surface roughness caused by the deposition of nanoparticles on the heating surface dominating the thermal resistance caused by the nanolayer. Moreover, the enhancement of the HTC is related to the increase of the surface roughness which in turn depends on the diameter of the nanoparticles deposited on the heating surface, this situation occurring when  $R_a/d_p > 1$ . Finally, another parameter that should be taking into account in the nanofluid pool boiling phenomenon is the boiling time effect, since the deposition of nanoparticles occurs during the bubble growth and departure from the heating surface - as the nanofluid boiling time increases, the nanolayer thickness also increases and causes the deterioration of the HTC.

#### 4. Conclusions

The following conclusions can be drawn from the present study:

- The pool boiling curves and the HTC observed for both smooth and rough heating surfaces boiled with DI water follow the general trend pointed out in the literature.
- By using nanofluids, it was observed a decrease in the wall superheating up to 32% and 12% for the SS and RS surfaces, respectively, for the same heat flux in comparison to that of DI water. This implies that a high heat flux can be achieved with relatively low wall superheating, and consequently improving the efficiency and safety of the thermal systems.
- For low concentration nanofluids subjected to moderate heat flux, appreciable enhancement of the HTC was observed for the smooth and rough surfaces as compared to DI water. It is argued that this phenomenon is related to the increase of the radius of the cavities due to changes in the morphology of the surface during the pool boiling of the nanofluid. For the rough surface, the HTC decreases drastically with increasing heat flux due to the intensification of the nanoparticle deposition rate, and the growth of the thermal resistance of the heating surface by the filling of the cavities with nanoparticles.

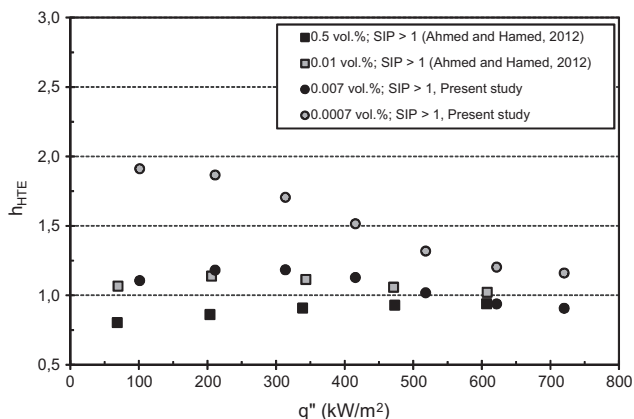


Fig. 13. Pool boiling heat transfer coefficient enhancement ratio as a function of heat flux, for the smooth surface ( $R_a = 0.05 \mu m$ ).

- Degradation of the boiling heat transfer with increasing heat flux was observed for high concentration nanofluids, regardless of the surface roughness. This behavior was observed to be more pronounced for rough surfaces.
- By comparing the HTC of nanofluids and DI water, it was observed for low nanofluids concentration at moderate heat flux an enhancement up to 75% for the smooth surface, and up to 15% for the rough surface.
- In general, the differences in the nanofluid pool boiling performance in terms of enhancement/deterioration of HTC observed by the various authors in Table 1 strongly depends on the morphology changes on the heating surface. The authors concluded that changes on the surface due to nanoparticle deposition increase the HTC only for low nanoparticle concentrations, and especially when the  $SIP > 1$ . Moreover, a higher nanoparticle deposition rate occurs for heat fluxes greater than  $400 \text{ kW/m}^2$ , this latter value being considered the upper limit of a moderate heat flux for nanofluid pool boiling.
- Finally, the analysis of the heat transfer enhancement ratio allowed concluding that the use of nanofluids is effective when applied to designed heating surfaces, granted that the nanofluid concentration is relatively low and the heat flux moderate (up to  $400 \text{ kW/m}^2$ ).

## Acknowledgments

The authors are grateful for the financial support from the PPGEM – UNESP/FEIS, from the National Counsel of Technological and Scientific Development of Brazil (CNPq grant number 458702/2014-5), from São Paulo Research Foundation – FAPESP (grant numbers 2013/15431-7 and 2014/19497-5) and from Coordination for the Improvement of Higher Education Personnel – CAPES sponsored postdoctoral fellowship for Mogaji T. S.

## References

- [1] J. Barber, D. Brutin, L. Tadrist, A review on boiling heat transfer enhancement with nanofluids, *Nanoscale Res. Lett.* 6 (2011) 280.
- [2] D. Ciloglu, A. Bolukbasi, A comprehensive review on pool boiling of nanofluids, *Appl. Therm. Eng.* 84 (2015) 45–63.
- [3] L.K. Nayara, H.F. Douglas, E.P. Bandarra Filho, A review on applications of nanofluids in automotive cooling system, Proceedings of ENCIT, in: 15th Brazilian Congress of Thermal Sciences and Engineering 2014 November 10–13, 2014, Belém, PA, Brazil.
- [4] S. Lee, S.U.S. Choi, S. Li, J.A. Eastman, Measuring thermal conductivity of fluids containing oxide nanoparticles, *ASME J. Heat Transf.* 121 (1999) 280–289.
- [5] J.A. Eastman, S.U.S. Choi, S. Li, W. Yu, L.J. Thompson, Anomalous increasing effective thermal conductivities of ethylene glycol-based nanofluid containing copper nanoparticles, *Appl. Phys. Lett.* 78 (2001) 718–720.
- [6] M. Kole, T.K. Dey, Thermal conductivity and viscosity of  $\text{Al}_2\text{O}_3$  nanofluid based on car engine coolant, *J. Phys. D Appl. Phys.* 43 (2010) 315501–315510.
- [7] Y.M. Xuan, Q. Li, Investigation on convective heat transfer and flow features of nanofluid, *ASME J. Heat Transf.* 125 (2003) 151–155.
- [8] D.S. Wen, Y.L. Ding, Experimental investigation into convective heat transfer of nanofluid at entrance area under laminar flow region, *Int. J. Heat Mass Transf.* 47 (2004) 5181–5188.
- [9] S.K. Das, N. Putra, P. Thiesen, W. Roetzel, Temperature dependence of thermal conductivity enhancement for nanofluids, *J. Heat Transf.* 125 (2003) 567.
- [10] O. Ahmed, M.S. Hamed, Experimental investigation of the effect of particle deposition on pool boiling of nanofluids, *Int. J. Heat Mass Transf.* 55 (2012) 3423–3436.
- [11] J. Buongiorno et al., A benchmark study on the thermal conductivity of nanofluids, *J. Appl. Phys.* 106 (2009) 094312.
- [12] N. Dinh, J. Tu, T. Theofanous, Hydrodynamic and physico-chemical nature of burnout in pool boiling, in: Proceedings of 5th Int. Conf. on Multiphase Flow, 2004, Yokohama, Japan.
- [13] D. Wen, Y. Ding, Experimental investigation into the pool boiling heat transfer of aqueous based  $\gamma$ -alumina nanofluids, *J. Nanoparticle Res.* 7 (2005) 265–274.
- [14] D. Wen, Y. Ding, R.A. Williams, Pool boiling heat transfer of aqueous  $\text{TiO}_2$ -based nanofluids, *J. Enhanc. Heat Transf.* 13 (2006) 231–244.
- [15] K.J. Park, D. Jung, Enhancement of nucleate boiling heat transfer using carbon nanotubes, *Int. J. Heat Mass Transf.* 50 (2007) 4499–4502.
- [16] Z.H. Liu, J.G. Xiong, R. Bao, Boiling heat transfer characteristics of nanofluids in a flat heat pipe evaporator with micro-grooved heating surface, *Int. J. Multiph. Flow* 33 (2007) 1284–1295.
- [17] M.A. Kedzierski, Effect of  $\text{CuO}$  Nanoparticle concentration on R134a/lubricant pool-boiling heat transfer, *ASME J. Heat Transf.* 131 (2009) 043205.
- [18] S.K. Das, N. Putra, W. Roetzel, Pool boiling characteristics of nano-fluids, *Int. J. Heat Mass Transf.* 46 (2003) 851–862.
- [19] I.C. Bang, S.H. Chang, Boiling heat transfer performance and phenomena of  $\text{Al}_2\text{O}_3$ -water nano-fluids from a plain surface in a pool, *Int. J. Heat Mass Transf.* 48 (2005) 2407–2419.
- [20] H.D. Kim, M.H. Kim, Effect of nanoparticle deposition on capillary wicking that influences the critical heat flux in nanofluids, *Appl. Phys. Lett.* 91 (2007) 014104.
- [21] V. Trisaksri, S. Wongwises, Nucleate pool boiling heat transfer of  $\text{TiO}_2$ -R141b nanofluids, *Int. J. Heat Mass Transf.* 52 (2009) 1582–1588.
- [22] G.P. Narayan, K.B. Anoop, S.K. Das, Mechanism of enhancement/deterioration of boiling heat transfer using stable nanoparticle suspensions over vertical tubes, *J. Appl. Phys.* 102 (2007) 074317.
- [23] K.J. Park, D.S. Jung, S.E. Shim, Nucleate boiling heat transfer in aqueous solutions with carbon nanotubes up to critical heat fluxes, *Int. J. Multiph. Flow* 35 (2009) 525–532.
- [24] S.M. Kwarik, R. Kumar, G. Moreno, J. Yoo, S.M. You, Pool boiling characteristics of low concentration nanofluids, *Int. J. Heat Mass Transf.* 53 (2010) 972–981.
- [25] Z. Shahmoradi, N. Etesami, M.N. Esfahany, Pool boiling characteristics of nanofluid on flat plate based on heater surface analysis, *Int. Commun. Heat Mass Transf.* 47 (2013) 113–120.
- [26] X. Tang, Y. Zhao, Y. Diao, Experimental investigation of the nucleate pool boiling heat transfer characteristics of  $\delta$ - $\text{Al}_2\text{O}_3$ -R141b nanofluids on a horizontal plate, *Exp. Therm. Fluid Sci.* 52 (2014) 88–96.
- [27] M.M. Sarafraz, F. Hormozi, Nucleate pool boiling heat transfer characteristics of dilute  $\text{Al}_2\text{O}_3$ -ethylene glycol nanofluids, *Int. Commun. Heat Mass Transf.* 58 (2014) 96–104.
- [28] M.M. Sarafraz, F. Hormozi, Pool boiling heat transfer to dilute copper oxide aqueous nanofluids, *Int. J. Therm. Sci.* 90 (2015) 224–237.
- [29] R. Kathiravan, R. Kumar, A. Gupta, R. Chandra, Preparation and pool boiling characteristics of copper nanofluids over a flat plate heater, *Int. J. Heat Mass Transf.* 53 (2010) 1673–1681.
- [30] J. H. Lee, T. Lee, Y.H. Jeong, Experimental study on the pool boiling CHF enhancement using magnetite-water nanofluids, *Int. J. Heat Mass Transf.* 55 (2012) 2656–2663.
- [31] S. Vafaei, Nanofluid pool boiling heat transfer phenomenon, *Powder Technol.* 277 (2015) 181–192.
- [32] M.M. Sarafraz, F. Hormozi, S.M. Peyghambarzadeh, Pool boiling heat transfer to aqueous alumina nano-fluids on the plain and concentric circular micro-structured (CCM) surfaces, *Exp. Therm. Fluid Sci.* 72 (2016) 125–139.
- [33] J.C. Maxwell, A Treatise on Electricity and Magnetism, first ed., Clarendon Press, Oxford, UK, 1873.
- [34] R.L. Hamilton, O.K. Crosser, Thermal conductivity of heterogeneous two-component systems, *Ind. Eng. Chem. Fundam.* 1 (1962) 187–191.
- [35] I.S. Kiyomura, L.L. Manetti, A.P. da Cunha, G. Ribatski, E.M. Cardoso, An analysis of the effects of nanoparticles deposition on characteristics of the heating surface and on pool boiling of water, *Int. J. Heat Mass Transf.* (2016).
- [36] B.N. Taylor, C.E. Kuyatt, Guidelines for Evaluating and Expressing the Uncertainty of NIST Measurement Results, NIST Technical Note 1297, Gaithersburg, 1994.
- [37] F.P. Netto, A.A.U. Moraes, U. Ribatski, The effects of the nanoparticle concentration and surface roughness on the contact angle of nanofluids, in: Proceedings of 22nd ABCM International Congress of Mechanical Engineering, Ribeirão Preto, Brazil, 2013.
- [38] W.M. Rohsenow, A method of correlating heat transfer data for surface boiling liquids, *Trans. ASME* 74 (1952) 969–976.
- [39] R.I. Vachon, G.H. Nix, G.E. Tanager, Evaluation of constants for the rohseonow pool-boiling correlation, *J. Heat Transf.* 90 (1968) 239.
- [40] K. Stephan, Heat Transfer in Condensation and Boiling, Springer-Verlag, Berlin, 1992.
- [41] W.M. Rohsenow, Boiling, *Annu. Rev. Fluid Mech.* 3 (1971) 211–236.
- [42] S.J. Kim, I.C. Bang, J. Buongiorno, L.W. Hu, Surface wettability change during pool boiling of nanofluids and its effect on critical heat flux, *Int. J. Heat Mass Transf.* 50 (2007).
- [43] C.H. Wang, V.K. Dhir, On the gas entrapment and nucleation site density during pool boiling of saturated water, *J. Heat Transf.* 115 (1993) 670.
- [44] P. Griffith, J.D. Wallis, The role of surface conditions in nucleate boiling, *Chem. Eng. Prog. Symp. Ser.* 56 (1960) 49–63.